The International Journal of Robotics Research

http://ijr.sagepub.com/

Argos: A Novel 3-DoF Parallel Wrist Mechanism

Peter Vischer and Reymond Clavel
The International Journal of Robotics Research 2000 19: 5
DOI: 10.1177/02783640022066707

The online version of this article can be found at: http://ijr.sagepub.com/content/19/1/5

Published by:

\$SAGE

http://www.sagepublications.com

On behalf of:



Multimedia Archives

Additional services and information for The International Journal of Robotics Research can be found at:

Email Alerts: http://ijr.sagepub.com/cgi/alerts

Subscriptions: http://ijr.sagepub.com/subscriptions

Reprints: http://www.sagepub.com/journalsReprints.nav

Permissions: http://www.sagepub.com/journalsPermissions.nav

Citations: http://ijr.sagepub.com/content/19/1/5.refs.html

>> Version of Record - Jan 1, 2000

What is This?

Peter Vischer Reymond Clavel

Institute of Robotic Systems Swiss Federal Institute of Technology 1015 Lausanne, Switzerland

Argos: A Novel 3-DoF Parallel Wrist Mechanism

Abstract

This article presents a novel parallel spherical mechanism called Argos with three rotational degrees of freedom. Design aspects of the first prototype built of the Argos mechanism are discussed. The direct kinematic problem is solved, leading always to four nonsingular configurations of the end effector for a given set of joint angles. The inverse-kinematic problem yields two possible configurations for each of the three pantographs for a given orientation of the end effector. Potential applications of the Argos mechanism are robot wrists, orientable machine tool beds, joy sticks, surgical manipulators, and orientable units for optical components. Another pantograph based new structure named PantoScope having two rotational DoF is also briefly introduced.

KEY WORDS—parallel robot, machine tool, 3 degree of freedom (DoF) wrist, pure orientation, direct kinematics, inverse kinematics, Pantograph based, Argos, PantoScope

1. Introduction

Parallel robots offer several advantages over serial robots, such as greater stiffness, a higher payload/weight ratio, reduced inertia, and higher precision. Disadvantages are lower dexterity, a smaller workspace, more singularities, and a more complex mathematical treatment.

Gough and Whitehall (1962) designed the first fully parallel, 6-DoF mechanism, which was used to test tires. Stewart (1965) proposed a similar mechanism for use as a flight simulator. In robotics, this concept has the disadvantage of low dexterity (small workspace, and small orientation range). In designing serial robots, it is convenient to separate the functionality positioning from that of orienting the gripper (Craig 1989). A serial manipulator is therefore usually composed of a positioning structure followed by an orienting structure (wrist). It is characteristic that the first concept of a parallel robot shows precisely this separation of functionalities (Pollard 1942). Pollard's design of a car-painting robot consists

The International Journal of Robotics Research Vol. 19, No. 1, January 2000, pp. 5-11, ©2000 Sage Publications, Inc.

of a 3-DoF structure that is capable of positioning a 2-DoF wrist in parallel. A slight disadvantage of Pollard's design is that the positioning structure's flange (which Pollard calls the "gun-carrying head," where the wrist is attached) changes its orientation during motion. In other words, the orientation of the gripper is coupled to its position.

This problem was overcome by Clavel (1985), who proposed a positioning structure (Delta) that maintains its flange's orientation with respect to the base. This concept has been patented and named the "spatial parallelogram," indicating that the flange (which Clavel terms the "nacelle") is subjected to pure translations only.

Either a serial or a parallel wrist can be affixed to the Delta's flange. A comprehensive study of robot wrists can be found in Rosheim's work (1989). However, to fix a wrist at the robot's flange partially destroys the advantage of a parallel robot having a low mobile mass and therefore low inertia. For this reason, it is more convenient to orient the machine bed with respect to the robot.

If it is to be highly dynamic, such a counterpart to the Delta robot should also have a low mobile mass. The search was therefore restricted to fully parallel structures having three rotational degrees of freedom. Unlike the solution chosen by Pollard (1942), the rotation center should be free of joints to fix the workpiece there. A manipulator fulfilling these claims was presented by Asada and Cor Granito (1985), and further investigated by Gosselin and colleagues (Gosselin and Angeles 1989; Gosselin, Sefrioui, and Richard 1992; Gosselin and Hamel 1994; Gosselin and Gagné 1995), who called it the Agile Eye. It is composed of three spherical chains built of three revolute joints (R-joints), each of which connects the base to the end effector (see also Cox and Tesar's work (1989)).

Recently, a second type of such a mechanism (see Fig. 1) was found, based on a new concept (Vischer 1995) and called Argos. This novel mechanism offers several advantages over existing 3(3R) spherical mechanisms such as the Agile Eye (Gosselin and Hamel 1994). The mechanical design of Argos is extremely simple since all joints of one kinematic chain lie in a plane. Connecting links are therefore easy to manufacture, and less link interference occurs during motion. The Argos mechanism is basically a spatial structure with its joints



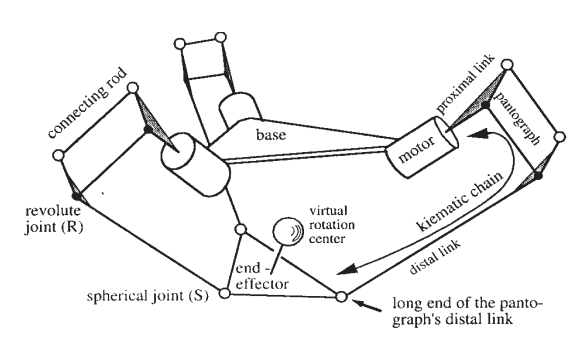


Fig. 1. The Argos mechanism.

arranged around a common center. Unlike real spherical structures, joint misalignments will not create supplementary reaction forces in the joints, which tend to yield a lower lifetime for the mechanism. The inverse kinematics for the 3R kinematic chain of a 3(3R) mechanism leads to two solutions, where the elbow is pointing to the right-hand side and the left-hand side, respectively. These two solutions cannot be as easily distinguished as the two solutions from the inverse problem of the Argos mechanism. An Argos-like mechanism with six motors, called HapticMaster, was proposed by Iwata (1995). It also uses pantographs, but is a fully spatial structure with 6 DoF and no virtual rotation center. In this article, a first prototype of Argos is presented, and its direct- and inversekinematic problems are solved. Furthermore, a mechanism that is closely related to Argos, called PantoScope, is also introduced.

2. The Basic Design

Figure 1 shows the Argos mechanism, which is a novel 3[R(2R/2S)S] design of a rotational parallel manipulator with 3 DoF. The end effector is connected to its base by three identical kinematic chains. Each chain is attached to the base plate by a revolute joint (R-joint) with its axis pointing to the virtual rotation center. Each axis carries a pantograph, which is a planar parallelogram equipped with four R-joints in its corners. To avoid static overdetermination in space, it is possible to replace one pair of R-joints by a pair of spherical joints (S-joints), as shown in Figure 1. The long end of the pantograph's distal link describes a sphere around the virtual rotation center. An S-joint links the pantograph to the end effector.

Two different kinds of motorizations are possible for a pantograph. The motor can either actuate the first R-joint (see Fig. 1), or, by means of conical gearwheels, the second R-joint. The first solution is easier to carry out, but the pantograph is subjected to bending stress. In the second case, the pantograph works in a push-pull mode, which is generally preferable. However, a detailed study of the second case has shown that the Argos mechanism remains in a singularity right at its nominal position (Vischer 1995). This is not the case for the first possibility of motorization, which will therefore be further discussed.

A criterion for the mobility (MO) of spatial multibody mechanisms can be found in the works of Hunt (1978) and Clavel (1991), which is a modified Grübler criterion:

$$MO = \sum MO_i - 6 \cdot bo, \tag{1}$$

where MOi stands for the degrees of freedom of each joint of the mechanism, and bo represents the number of independent loops.

Applying eq. (1) to the Argos mechanism shows that for a connecting rod equipped with its two S-joints (see Fig. 1), only five instead of six degrees of freedom must be counted. This is because the connecting rod can be turned around its longitudinal axis without influencing the pose of the end effector representing an isolated degree of freedom. For the calculation, one of the S-joints can be considered as a universal joint blocking off the isolated degree of freedom,

$$MO = 3 \cdot (1 + 2 + 5 + 3) - 6 \cdot 5 = 3.$$
 (2)

Equation (2) leads indeed to the expected 3 DoF for the Argos mechanism.

3. Prototype

According to Gosselin, Sefrioui, and Richard (1992), the direct problem of a general 3-DoF parallel wrist has at most eight solutions. By arranging the motor axis as well as the vector pointing from the virtual rotation center to the end-effector's S-joints orthogonal to each other, a closed-form solution can be found (Gosselin and Gagné 1995). This orthogonal design has the further advantage of being optimal with respect to workspace and singularities. The workspace covers the entire sphere, and is therefore theoretically infinite (Gosselin and Angeles 1989). The singularities are located far away from the nominal position. Unfortunately, the virtual rotation center is surrounded by the mechanism, which renders the access more difficult. However, since the goal of the first prototype (see Fig. 2) was to study and calibrate these kinds of mechanisms, the orthogonal design was chosen (Vischer 1996). The virtual rotation center is indicated by the white ball in the center of Figure 2.

The workspace of the prototype shown in Figure 2 is about $\pm 60^{\circ}$ for all three orientation angles. Such a large workspace was possible by designing S-joints with a cone angle of $\pm 60^{\circ}$. Furthermore, the conventional design of a pantograph as shown in Figure 3 was replaced by an original steel-cable design, which is shown in Figure 4.

The conventional design (see Fig. 3) has a singularity with zero stiffness when the parallelogram joins the antiparallelogram (Dijksman 1976). On the other hand, the stiffness of

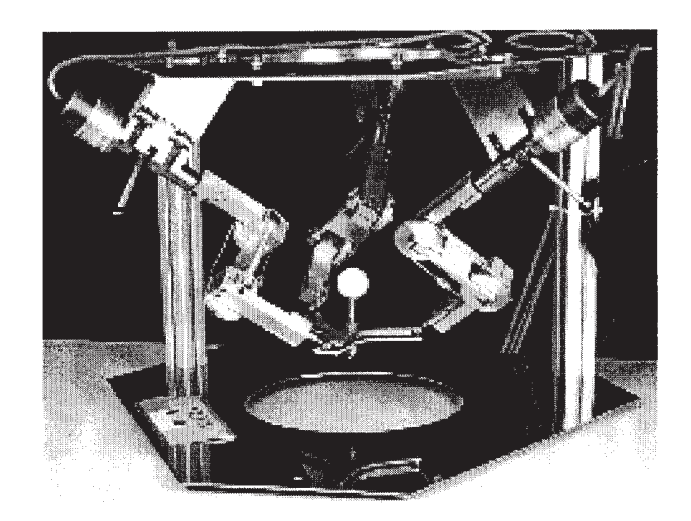


Fig. 2. Prototype of the Argos mechanism.

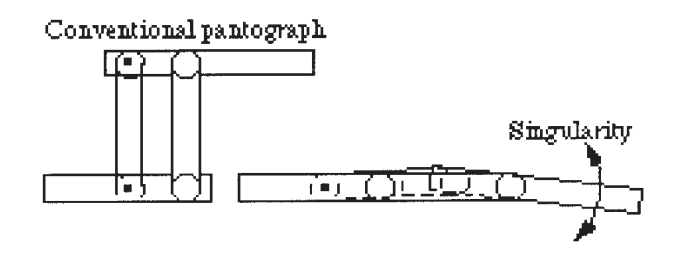


Fig. 3. Conventional pantograph with singularity.

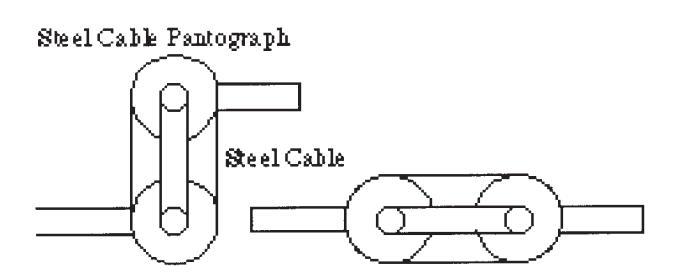


Fig. 4. Steel-cable pantograph without singularity.

the steel-cable design (see Fig. 4) remains constant within the full circle. As a further advantage, only two (rather than four) R-joints are required.

Constant stiffness of the pantographs is advantageous for the Argos mechanism because of their travel range of more than $\pm 60^{\circ}$. To increase stiffness, the steel cable can be replaced by a steel strip.

4. Parameterization

Figure 5 shows the parameterization of the Argos mechanism. The virtual rotation center is chosen as the origin for the base frame {b} as well as for the moving frame {p}. The parameterization is independent of the size of the Argos mechanism, due to a projection on the unit sphere about the virtual rotation center.

Unit vectors \mathbf{w}_i directed along the motor axes include

$${}^{b}\mathbf{w}_{1} = \{1, 0, 0\}^{T},$$

$${}^{b}\mathbf{w}_{2} = \{0, 1, 0\}^{T},$$

$${}^{b}\mathbf{w}_{3} = \{0, 0, 1\}^{T}.$$
(3)

Unit vectors \mathbf{u}_i perpendicular to the pantograph planes (First pantograph: x-z plane, second and third pantograph: y-z plane; see Fig. 5) are represented by

$$b^{b}\mathbf{u}_{1} = \operatorname{Rot}(x, \alpha_{1}) \cdot \{0, 1, 0\}^{T},$$

$$b^{b}\mathbf{u}_{2} = \operatorname{Rot}(y, \alpha_{2}) \cdot \{-1, 0, 0\}^{T},$$

$$b^{b}\mathbf{u}_{3} = \operatorname{Rot}(z, \alpha_{3}) \cdot \{-1, 0, 0\}^{T}.$$
(4)

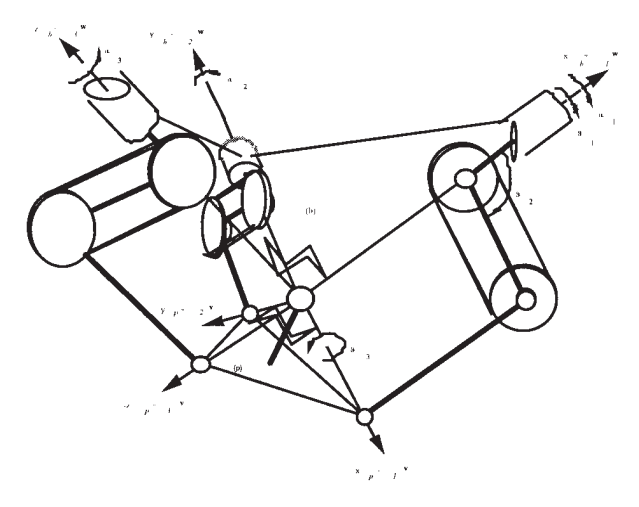


Fig. 5. Parameterization.

Unit vectors \mathbf{v}_i pointing to the S-joints include

$${}^{p}\mathbf{v}_{1} = \{1, 0, 0\}^{T},$$

$${}^{p}\mathbf{v}_{2} = \{0, 1, 0\}^{T},$$

$${}^{p}\mathbf{v}_{3} = \{0, 0, -1\}^{T}.$$
(5)

The transformation between the $\{b\}$ and $\{p\}$ frames is a pure rotation \mathbf{R} , which may be described with three Euler angles. However, there exist 12 different sets of Euler angles, and the right choice is very important.

The solvability of the direct problem depends strongly on the chosen set. Here, we use the results of Gosselin (1995), who proposed to introduce the Euler angles in such a way that the first Euler angle coincides with the first motor angle,

$${}_{b}^{p}\mathbf{R} = \operatorname{Rot}(x, \vartheta_{1}) \cdot \operatorname{Rot}(y, \vartheta_{2}) \cdot \operatorname{Rot}(x, \vartheta_{3}). \tag{6}$$

The closure equations can then be derived using the orthogonality of the \mathbf{u}_i and \mathbf{v}_i vectors. In other words, the \mathbf{v}_i vectors must be located in the pantograph plans as follows:

$${}^{b}\mathbf{u}_{i}^{T} \cdot {}_{b}^{p}\mathbf{R} \cdot {}^{p}\mathbf{v}_{i} = 0, \quad i = 1 \dots 3.$$
 (7)

Expansion of eq. (7) leads to the following system of equations, which is free of design parameters:

$$\sin \vartheta_2(\sin \vartheta_1 \cos \alpha_1 - \cos \vartheta_1 \sin \alpha_1) = 0, \tag{8}$$

 $-\sin\vartheta_2\sin\vartheta_3\cos\alpha_2 +$

$$(\sin \vartheta_1 \cos \vartheta_3 + \cos \vartheta_1 \cos \vartheta_2 \sin \vartheta_3) \sin \alpha_2 = 0, \quad (9)$$

 $\sin \vartheta_2 \cos \vartheta_3 \cos \alpha_3 -$

$$(\cos \vartheta_1 \sin \vartheta_3 + \sin \vartheta_1 \cos \vartheta_2 \cos \vartheta_3) \sin \alpha_3 = 0. \quad (10)$$

5. Solving the Direct Problem

The direct problem consists of finding, for a given set of motor angles, zero, one, or several sets of Euler angles $\alpha_1, \alpha_2, \alpha_3 \rightarrow \vartheta_1, \vartheta_2, \vartheta_3$. The nonlinear system of equations (eqs. (8), (9), and (10)) is coupled in the variables ϑ_i , which is typical for the direct problem of parallel robots.

Due to the careful choice of the Euler angles (eq. (6)), eq. (8) can be rewritten as

$$\sin \vartheta_2 \sin(\vartheta_1 - \alpha_1) \tag{11}$$

To satisfy eq. (11) either the first or the second factor can be zero, which leads to two different cases.

5.1. The First Case: $\sin(\vartheta_1 - \alpha_1) = 0$

Solving for ϑ_1 leads to $\vartheta_{1_{1,2}} = \alpha_1, \alpha_1 + \pi$. However, the second solution can be dropped, since the description of the

orientation becomes redundant. In other words, the Euler angle set $(\alpha_1 + \pi, -\vartheta_2, \pi)$ would describe the same orientation of the end effector with respect to the base as the Euler angle set $(\alpha_1, \vartheta_2, 0)$, hence

$$\vartheta_1 = \alpha_1. \tag{12}$$

A rearrangement of the remaining two equations (eqs. (9) and (10)) leads to

$$I_1 \cos \vartheta_3 + I_2 \sin \vartheta_3 = 0,$$

$$J_1 \cos \vartheta_3 + J_2 \sin \vartheta_3 = 0,$$
(13)

with

$$I_{1} = \sin \alpha_{1} \sin \alpha_{2},$$

$$I_{2} = -\cos \alpha_{2} \sin \vartheta_{2} + \cos \alpha_{1} \sin \alpha_{2} \cos \vartheta_{2},$$

$$J_{1} = \cos \alpha_{3} \sin \vartheta_{2} - \sin \alpha_{1} \sin \alpha_{3} \cos \vartheta_{2},$$

$$J_{2} = -\cos \alpha_{1} \sin \alpha_{3}.$$

$$(14)$$

The condition for the system of eq. (13) to be fulfilled identically is that the determinant of their factors vanishes:

$$I_1 J_2 - I_2 J_1 = 0. (15)$$

Expanding and rearranging the result leads to

$$\sin \vartheta_2(C_1 \cos \vartheta_2 + C_2 \sin \vartheta_2) = 0, \tag{16}$$

with

$$C_1 = -\cos \alpha_1 \sin \alpha_2 \cos \alpha_3 - \sin \alpha_1 \cos \alpha_2 \sin \alpha_3,$$

$$C_2 = \cos \alpha_2 \cos \alpha_3 - \cos \alpha_1 \sin \alpha_1 \sin \alpha_2 \sin \alpha_3.$$
(17)

As mentioned earlier, the case where the first factor of eqs. (11) and (16) is zero will be treated in the next subsection. The second factor of eq. (16) is thus set to zero, and is solved for the second Euler angle. Back substitution into the first part of eq. (13) leads to the first set of solutions of the direct problem of the Argos mechanism. It always has four solutions:

$$\vartheta_1 = \alpha_1$$

$$\vartheta_{2_{1,2}} = \arctan 2(\pm C_1, \mp C_2)$$

$$\vartheta_{3_{1,4}} = \arctan 2(\pm I_1, \mp I_2(\vartheta_{2_{1,2}})).$$
(18)

To illustrate the result described by eq. (18), all four sets of Euler angles that correspond to the motor-angle set $(45^{\circ}, -45^{\circ}, 45^{\circ})$ were calculated. This set represents the nominal position of the Argos mechanism, which is shown in the lower-right corner of Figure 6. The remaining three configurations are identical with respect to the three symmetrical planes of the Argos mechanism.

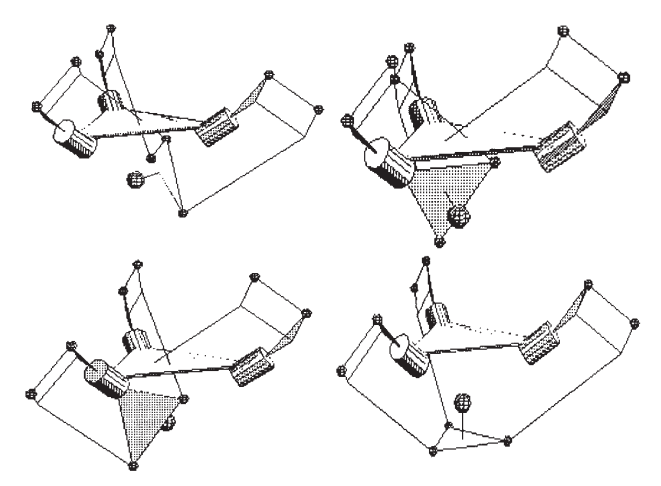


Fig. 6. The first set of solutions for the direct problem.

5.2. The Second Case: $\sin \vartheta_2 = 0$

Solving for ϑ_2 leads to

$$\vartheta_{2_{1,2}} = 0, \pi. \tag{19}$$

The rotation matrix (eq. (6)) reduces to

$$\mathbf{R}_{0,\pi} = \begin{bmatrix} \pm 1 & 0 & 0\\ 0 & \cos(\vartheta_1 \pm \vartheta_3) & \mp \sin(\vartheta_1 \pm \vartheta_3)\\ 0 & \sin(\vartheta_1 \pm \vartheta_3) & \pm \cos(\vartheta_1 \pm \vartheta_3) \end{bmatrix}, (20)$$

whereas eq. (9) or (10) is reduced to

$$\vartheta_1 \pm \vartheta_3 = 0, \pi. \tag{21}$$

Equations (20) and (21) yield the following four rotation matrices:

$$\mathbf{R}_{1} = \begin{bmatrix} 1 & 0 & 0 \\ 0 & 1 & 0 \\ 0 & 0 & 1 \end{bmatrix}, \quad \mathbf{R}_{2} = \begin{bmatrix} -1 & 0 & 0 \\ 0 & 1 & 0 \\ 0 & 0 & -1 \end{bmatrix},$$

$$\mathbf{R}_{3} = \begin{bmatrix} 1 & 0 & 0 \\ 0 & -1 & 0 \\ 0 & 0 & -1 \end{bmatrix}, \quad \mathbf{R}_{4} = \begin{bmatrix} -1 & 0 & 0 \\ 0 & -1 & 0 \\ 0 & 0 & 1 \end{bmatrix}.$$
(22)

These four solutions exist always, and are independent of the given motor angles. In fact, if one of the S-joints lies on its corresponding motor axis, the pantograph can be freely twisted without influencing the orientation of the end effector, which is an inverse singularity. If orientations exist, where all three S-joints lie on their corresponding motor axes, any set of motor angles can be freely imposed. By looking at eq. (22), it can be seen that four such orientations exist. Figure 7 shows the orientations corresponding to the four rotation matrices given in eq. (22).

In the work of Gosselin, Sefrioui, and Richard (1992), a polynomial of the eighth order was found as the solution to

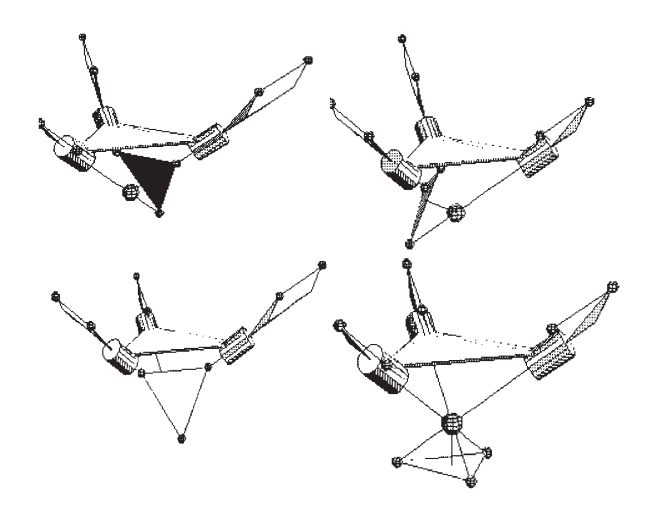


Fig. 7. The second set of solutions for the direct problem.

the direct problem of a general parallel wrist. However, as Gosselin and Gagné (1995) have shown, this general solution can be simplified considerably if an orthogonal design for the mechanism is chosen. The problem decomposes into four real, individual solutions (eq. (18) and Fig. 6) and four stationary solutions (eq. (22) and Fig. 7) located at inverse singularities.

6. Solving the Inverse Problem

The inverse problem consists of finding, for a given set of Euler angles, zero, one, or several sets of motor angles, $\vartheta_1, \vartheta_2, \vartheta_3 \rightarrow \alpha_1, \alpha_2, \alpha_3$. The nonlinear system of equations (eqs. (8), (9), and (10)) is decoupled in the variables (α_i) , which is typical for the inverse problem of parallel robots:

$$a_i \cos(\alpha_i + b_i \sin(\alpha_i = 0, \quad i = 1...3.$$
 (23)

with

$$a_{1} = \sin \vartheta_{1} \sin \vartheta_{2},$$

$$b_{1} = -\cos \vartheta_{1} \sin \vartheta_{2},$$

$$a_{2} = -\sin \vartheta_{2} \sin \vartheta_{3},$$

$$b_{2} = \sin \vartheta_{1} \cos \vartheta_{3} + \cos \vartheta_{1} \cos \vartheta_{2} \sin \vartheta_{3},$$

$$a_{3} = \sin \vartheta_{2} \cos \vartheta_{3},$$

$$b_{3} = -\cos \vartheta_{1} \sin \vartheta_{3} - \sin \vartheta_{1} \cos \vartheta_{2} \cos \vartheta_{3}.$$

$$(24)$$

Equation (23) can now be solved for the unknown joint angle, yielding always two solutions per joint-link train:

$$\alpha_{i_{1,2}} = \arctan 2(\pm a_i, \mp b_i), i = 1.3.$$
 (25)

Figure 8 shows the two different solutions for one of the pantographs. For the Argos prototype (Fig. 2), the passive R-joints can only move within a range of 0 to π . Thus, only the first solution is reachable within the limitations of the joints.

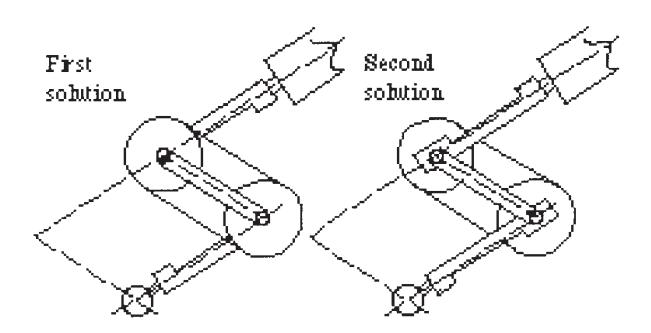


Fig. 8. The two solutions of the inverse problem.

Distinction of the first and second solutions is based on the \mathbf{w}_i , \mathbf{u}_i , and \mathbf{v}_i vectors having to build for the first and second joint-link train a left-handed system, and for the third joint-link train a right-handed system. The constraint can be expressed by means of the triple product:

$$\begin{array}{l} \text{left-handed}: & (\boldsymbol{w}_1 \times \boldsymbol{u}_1) \cdot \boldsymbol{v}_1 < 0, \\ & (\boldsymbol{w}_2 \times \boldsymbol{u}_2) \cdot \boldsymbol{v}_2 < 0, \end{array} \tag{26}$$

right-handed:
$$(\mathbf{w}_3 \times \mathbf{u}_3) \cdot \mathbf{v}_3 > 0.$$
 (27)

Expansion yields

$$b_1 \cos(\alpha_1) - a_1 \sin(\alpha_1) < 0,$$

 $b_2 \cos(\alpha_2) - a_2 \sin(\alpha_2) < 0,$ (28)
 $b_3 \cos(\alpha_3) - a_3 \sin(\alpha_3) > 0.$

Together with eq. (25), eq. (28) leads to a unique solution for the inverse problem of the Argos mechanism:

$$\alpha_1 = \arctan 2(a_1, -b_1),$$
 $\alpha_2 = \arctan 2(a_2, -b_2),$
 $\alpha_3 = \arctan 2(-a_3, b_3).$
(29)

7. Conclusions

A novel parallel mechanism with 3 DoF named Argos was presented in this paper and its functionality was verified by building a prototype. The direct- as well as the inverse-kinematic problem was solved in a closed form, both having eight solutions. A simple criterion allows us to reduce the number of solutions of the inverse-kinematic problem to a unique solution.

Potential applications include a robot wrist, an orientable machine tool bed, a joy stick, a surgical force-feedback manipulator, and an orientable unit for cameras and optical components. However, from a practical point of view, the application fields may be limited, since the Argos mechanism does

not provide the possibly of turning the gripper more the $\pm 60^{\circ}$ about its longitudinal axis (roll angle). In most industrial applications, the roll angle must be infinite.

To overcome this problem, 1 DoF was removed from the Argos mechanism. This led to another novel structure (see Fig. 9), called the PantoScope (Vischer 1995). For an infinite roll angle, a rotating actuator must be added to the end effector, leading to a hybrid 3-rotational-DoF mechanism.

To avoid static overdetermination in space, one pantograph must be omitted. An application of the PantoScope as a force-feedback manipulator for laparoscopic surgery was shown by Baumann, Glauser, and Tappy (1996). For a more detailed discussion of the PantoScope mechanism, including its direct-and inverse-kinematic models, the reader is referred to Vischer's (1995) work. Somewhat similar to the PantoScope is the CMS joint described by Hamlin and Sanderson (1994). However, the PantoScope is proposed as a fully motorized parallel robot, whereas the passive CMS joint was designed to overcome a problem arising if two S-joints coincide.

The motivation to build a prototype of the Argos and to investigate its kinematic properties also arose from a theoretical point of view: the Argos structure with its three rotational degrees of freedom can be regarded as a counterpart to the Delta robot with its three translational degrees of freedom. This not only concerns the degrees of freedom, but also the entire kinematic treatment. Investigation of the Argos mechanism therefore also provides more inside knowledge about the Delta robot. As an example, the accuracy of the end-effector's pose (position and orientation) is taken. For the Argos prototype shown in Figure 2, a position error of about 1 mm and an orientation error of about 1.5° was measured by means of three linear digital touch probes (TESA-GT130) and three gimbal-mounted encoders (Pewatron-PHE-20). For a Delta robot of comparable size, these errors are within 0.5 mm and 0.5°. The orientation error of the Argos mechanism can be eliminated by calibration, whereas for the Delta robot, it is the position error that shows the diametric opposite of the two mechanisms. This kind of pose improvement is possible with an extended nominal model. For a better prediction of the remaining three degrees of freedom (for the Argos, it is the

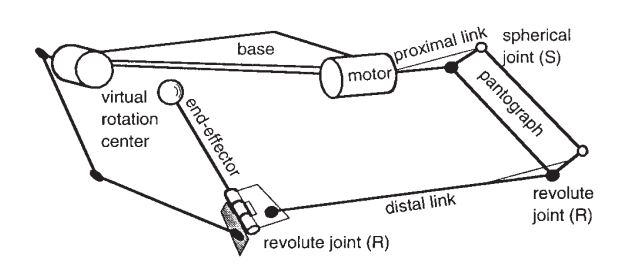


Fig. 9. The PantoScope mechanism.

position of the virtual rotation center, whereas for the Delta, it is the end-effector orientation), a much more complicated geometric model is needed for both structures. Readers interested in more detailed treatment of this subject are referred to Vischer's (1996) work, where both of the mechanisms were calibrated.

Acknowledgment

This research was financed by a scholarship promoting the exchange between the two Swiss Federal Institutes of Technologies, ETHZ and EPFL.

References

- Asada, H., and Cor Granito, J. A. 1985 (St. Louis, MO). Kinematic and static characterization of wrist joints and their optimal design. *Proc. of the IEEE Intl. Conf. on Robot. and Automat.* Los Alamitos, CA: IEEE, pp. 244–250.
- Baumann, R., Glauser, D., and Tappy, D. 1996 (San Diego, CA). Force feedback for virtual reality based minimally invasive surgery simulator. *Proc. of Med. Meets Virtual Reality*, vol. 4, pp. 564–579.
- Clavel, R. 1985. Device for the displacement and the positioning of an element in space, Swiss patent n° 672089 A5. (Dispositif pour le déplacement et le positionnement d'un élément dans l'espace. Brevet Suisse 672089 A5).
- Clavel, R. 1991. Conception d'un robot paralléle rapide à 4 degrés de liberté. PhD thesis, document 925, Ecole Polytechique fédérale de Lausanne (EPFL).
- Cox, D. and Tesar, D. 1989 (Columbus, OH). The dynamic model of a three degree of freedom parallel robotic Schoulder model. *Proc. of the 4th ICAR*, pp. 475–487.
- Craig, J. J. 1989. *Introduction to Robotics: Mechanics and Control*, 2nd ed. Reading, MA: Addision-Wesley.
- Dijksman, E. A. 1976. *Motion Geometry of Mechanisms*. Cambridge University Press.
- Gosselin, C. M., and Angeles, J. 1989. The optimum kinematic design of a spherical 3-DOF parallel manipulator.

- ASME J. Mech. Trans. Automat. Design 111:202–207.
- Gosselin, C. M., and Gagné, M. 1995. A closed-form solution for the direct kinematics of a special class of spherical three-degree of freedom parallel manipulators. In Merlet, J. P., and Ravani, B. (eds.): *Computational Kinematics*. Boston, MA: Kluwer Academic, pp. 231–240.
- Gosselin, C. M., and Hamel, J. F. 1994 (San Diego, CA,). The Agile Eye: A high-performance three-degree-of-freedom camera-orienting device. *Proc. of the IEEE Intl. Conf. on Robot. and Automat.*, vol. 1. Washington, DC: IEEE, pp. 781–786.
- Gosselin, C. M., Sefrioui, J., and Richard, M. J. 1992 (Scottsdale, AZ). On the direct kinematics of general spherical three-degree-of-freedom parallel manipulators. *Proc. of Robotics, Spatial Mechanisms, and Mechanical Systems: ASME 22nd Biennial Mechanisms Conf.*, vol. 45. New York: ASME, pp. 7–11.
- Gough, V. E., and Whitehall, S. G. 1962. Universal tyre test machine. *Proc. of the Ninth Intl. Tech. Congress, FISITA* (*Institution of Mechanical Engineers*).
- Hamlin, G. J., and Sanderson, A. C. 1994 (San Diego, CA). A novel concentric multilink spherical joint with parallel robotics applications. *Proc. of the IEEE Intl. Conf. on Robot. and Automat.*, vol. 2. Washington, DC: IEEE, pp. 1267–1272.
- Hunt, K. H. 1978. Kinematic Geometry of Mechanisms. Oxford, UK: Oxford Calderon Press.
- Iwata, H. 1995. HapticMaster. *Virtual Reality News* 4(6):27.Pollard, W. L. W. 1942. Position-controlling apparatus. United States Patent Office.
- Rosheim, M. E. 1989. *Robot Wrist Actuators*. New York: Wiley.
- Stewart, D. 1965. A platform with six degrees of freedom. *Proc. Institution Mech. Eng.* 180/1(15):371–386.
- Vischer, P. 1995. Argos: A novel parallel spherical structure. Technical Report 95-03, Ecole Polytechique fédérale de Lausanne (EPFL).
- Vischer, P. 1996. Improving the accuracy of parallel robots. PhD thesis, document 1570, Ecole Polytechique fédérale de Lausanne (EPFL).